



OPEN ACCESS

EDITED BY

Ulrike Stein,
Charité University Medicine Berlin,
Germany

REVIEWED BY

Jia Li,
University of North Carolina at Charlotte,
United States
Chen Ling,
Fudan University, China

*CORRESPONDENCE

Radhika Nair
✉ radhikanair@chg.res.in

†PRESENT ADDRESS

Radhika Nair,
Centre for Human Genetics,
Bangalore, India

RECEIVED 29 May 2023

ACCEPTED 24 August 2023

PUBLISHED 29 September 2023

CITATION

Thankamony AP, Ramkomuth S,
Ramesh ST, Murali R, Chakraborty P,
Karthikeyan N, Varghese BA, Jaikumar VS,
Jolly MK, Swarbrick A and Nair R (2023)
Phenotypic heterogeneity drives differential
disease outcome in a mouse model of
triple negative breast cancer.
Front. Oncol. 13:1230647.
doi: 10.3389/fonc.2023.1230647

COPYRIGHT

© 2023 Thankamony, Ramkomuth, Ramesh,
Murali, Chakraborty, Karthikeyan, Varghese,
Jaikumar, Jolly, Swarbrick and Nair. This is an
open-access article distributed under the
terms of the [Creative Commons Attribution
License \(CC BY\)](https://creativecommons.org/licenses/by/4.0/). The use, distribution or
reproduction in other forums is permitted,
provided the original author(s) and the
copyright owner(s) are credited and that
the original publication in this journal is
cited, in accordance with accepted
academic practice. No use, distribution or
reproduction is permitted which does not
comply with these terms.

Phenotypic heterogeneity drives differential disease outcome in a mouse model of triple negative breast cancer

Archana P. Thankamony^{1,2}, Sonny Ramkomuth³,
Shikha T. Ramesh^{1,2}, Reshma Murali¹, Priyanka Chakraborty⁴,
Nitheesh Karthikeyan¹, Binitha Anu Varghese¹,
Vishnu Sunil Jaikumar¹, Mohit Kumar Jolly⁴,
Alexander Swarbrick^{3,5} and Radhika Nair^{1,6*†}

¹Rajiv Gandhi Centre for Biotechnology, Trivandrum, Kerala, India, ²Manipal Academy of Higher Education (MAHE), Manipal, Karnataka, India, ³The Kinghorn Cancer Centre and Cancer Research Theme, Garvan Institute of Medical Research, Darlinghurst, NSW, Australia, ⁴Centre for BioSystems Science and Engineering, Indian Institute of Science, Bangalore, India, ⁵St Vincent's Clinical School, Faculty of Medicine, UNSW Sydney, Darlinghurst, NSW, Australia, ⁶Centre for Human Genetics, Bangalore, India

The triple negative breast cancer (TNBC) subtype is one of the most aggressive forms of breast cancer that has poor clinical outcome and is an unmet clinical challenge. Accumulating evidence suggests that intratumoral heterogeneity or the presence of phenotypically distinct cell populations within a tumor play a crucial role in chemoresistance, tumor progression and metastasis. An increased understanding of the molecular regulators of intratumoral heterogeneity is crucial to the development of effective therapeutic strategies in TNBC. To this end, we used an unbiased approach to identify a molecular mediator of intratumoral heterogeneity in breast cancer by isolating two tumor cell populations (T1 and T2) from the 4T1 TNBC model. Phenotypic characterization revealed that the cells are different in terms of their morphology, proliferation and self-renewal ability *in vitro* as well as primary tumor formation and metastatic potential *in vivo*. Bioinformatic analysis followed by Kaplan Meier survival analysis in TNBC patients identified Metastasis associated colon cancer 1 (Macc1) as one of the top candidate genes mediating the aggressive phenotype in the T1 tumor cells. The role of Macc1 in regulating the proliferative phenotype was validated and taken forward in a therapeutic context with Lovastatin, a small molecule transcriptional inhibitor of Macc1 to target the T1 cell population. This study increases our understanding of the molecular underpinnings of intratumoral heterogeneity in breast cancer that is critical to improve the treatment of women currently living with the highly aggressive TNBC subtype.

KEYWORDS

intratumoral heterogeneity, TNBC, MACC1, phenotypic heterogeneity, Lovastatin

1 Introduction

Breast cancer is a highly heterogeneous disease and displays considerable diversity among patients (intertumoral heterogeneity) as well as within a tumor (intratumoral heterogeneity) (1, 2). The differences in the expression of hormonal receptors (ER/PR), human epidermal growth factor receptor 2 (HER2), Ki67 proliferation index and gene expression profiles among patients has enabled the classification of breast cancer into distinct subtypes: Luminal A, Luminal B, HER2 + and TNBC (1–4). The TNBC subtype constitutes 10–20% of all breast cancer cases (5–8) and is defined by the lack of expression of ER, PR and HER2 receptors (9–12). Consequently, patients with TNBC do not respond to hormonal or anti-HER2 therapies (13). Currently there are no molecular targeted therapies against TNBC and chemotherapy is the mainstay treatment option (8). Unfortunately, only 20% of TNBC cases respond to conventional chemotherapy (13) and is characterized by aggressive clinical course with cerebral and visceral metastasis. Compared to other subtypes, TNBC patients show significantly poor prognosis and lower overall survival (14, 15) making it imperative to devise new therapeutic strategies for targeting the disease.

Although TNBC is treated as a single clinical entity, recent genomic, transcriptomic and proteomic characterization has revealed profound heterogeneity with in TNBC (12, 16–20). Based on gene expression profiling, TNBC can be further classified into distinct molecular subtypes that have unique biological features and varied response to chemotherapy (21–24). Intratumoral heterogeneity refers to the presence of distinct cell populations within the same tumor with varying genetic, morphologic and phenotypic characteristics (25–28). This heterogeneity could arise as a consequence of cell intrinsic factors like genetic or epigenetic alterations, along with cell extrinsic or microenvironmental fluctuations (13). Intratumoral heterogeneity is regarded as a major driver of tumor progression, therapeutic resistance and metastasis (18, 29). Hence, increased understanding of the molecular mechanisms underlying this phenomenon is key for efficient therapeutic targeting of the TNBC subtype (30).

Accumulating evidences suggest that distinct cell populations derived from the triple negative breast cancer display varied tumor growth and metastatic potential (27, 29, 31). Various studies have shown that distinct tumor cell populations may also cooperate to promote tumor aggressiveness in breast cancer (31–33). For instance, Martin-Pardillos et al. isolated several clonal cell populations from the MDA-MB-231 TNBC cell line by marking different clones using fluorescent proteins (33). They found that some clones were able induce aggressiveness in other clones through soluble factors, extracellular vesicles or physical interactions. Another study by Kuiken et al. has shown that distinct clonal subpopulations derived from a human TNBC cell line MDA-MB-468 displayed significant functional heterogeneity and also varied in their growth dynamics under different contexts (34). These studies point to the importance of isolating heterogeneous tumor cell subpopulations from bulk cancers in

order to unravel the molecular trappings underlying this phenomenon.

In order to dissect this further, we decided to investigate the 4T1 cell line, a widely used model system for studying TNBC heterogeneity. We were intrigued by an earlier study by Xiang et al. who observed two morphologically distinct tumor cell types following the *in vitro* culture of 4T1 primary tumor and lung metastases (35). One cell type displayed typical epithelial morphology while the other cell type was round and loosely touching the surrounding cells. However, these cells were not separately isolated or phenotypically characterized and the contribution of these two morphologically distinct tumor cells towards disease outcome was also not studied thoroughly. We have now successfully isolated two distinct tumor cell types from the primary tumor of the 4T1 model system (T1 and T2) which exhibited different *in vitro* phenotypes as well as *in vivo* disease outcomes (36). We further employed an unbiased transcriptomic analysis of the two cell populations in order to identify the key mediator of this phenotypic heterogeneity, thus opening up exciting new avenues to explore targeting of aggressive subpopulations of cells within a tumor.

2 Materials and methods

2.1 Cell culture

Mouse breast cancer cell line, 4T1, stably expressing green fluorescent protein (4T1GFP) was cultured in RPMI 1640 (11875119, Thermo Fischer Scientific) supplemented with 10% FBS (10270106, Thermo Fischer Scientific), Penicillin (100 Units/mL)/Streptomycin (100µg/mL) (15070063, Thermo Fischer Scientific), 0.25% (v/v) D+ Glucose (G8644, Sigma Aldrich), 1mM sodium pyruvate and 20mM HEPES. The primary cells were cultured in DMEM/F-12 (11320082, Thermo Fisher Scientific) supplemented with 10% FBS and Penicillin (100 Units/mL)/Streptomycin (100µg/mL). All the cells were grown in 5% CO₂ incubator at 37°C.

2.2 *In vivo* 4T1GFP tumor model

All animal experiments were conducted in accordance with RGCB institutional animal ethics committee. In order to generate 4T1GFP spontaneous metastasis model 7×10^3 4T1GFP cells were injected into the fourth mammary fat pad of six to eight weeks old BALB/c mice. For the resection experiment, the primary tumor was surgically removed when the tumor reached 0.8 cm³ volume. For experimental metastasis assay, 5×10^5 T1 and T2 cells in 100 µL DPBS were injected via tail vein (n=5). At ethical end point (as indicated by reduction in body weight and acute respiratory stress), mice were sacrificed and lung metastases were harvested. For long term survival analysis, mice were orthotopically injected with 7×10^3 T1 and T2 cells (n=5 and n=9 respectively). Survival analysis was performed using GraphPad Prism software.

2.3 Tumor dissociation and flow cytometric analysis of cell populations

Tumors harvested from the mice were dissociated into single cell suspension for FACS sorting. Tumor dissociation into single cell suspension was carried out using the MACS mouse Tissue Dissociation Kit (Miltenyi Biotec, USA) using manufacturer's protocols. Following the dissociation 1×10^6 tumor cells were washed once with DPBS with salts. The cells were then incubated in FcR blocking reagent (130-092-575, Miltenyi Biotec, USA) for 10 minutes on ice. After incubation, the cells were washed twice using DPBS with salts. Cells were stained for 20 minutes on ice with fluorochrome conjugated antibodies against lineage markers EpCam-FITC (130-102-995, Miltenyi Biotec, USA), CD140a-PE (130-102-502, Miltenyi Biotec, USA). Prior to analysis the cells were washed twice and resuspended in FACS buffer (DPBS with salts + 20% FBS + 20% HEPES). The stained tumor cells were analyzed using the flow cytometer (BD FACS Aria III, BD Biosciences, San Jose, CA, USA).

2.4 Cell proliferation assay

5×10^2 T1 and T2 tumor cells were seeded into 96 well plates and the cell proliferation were measured for 72 hours using MTT (3-(4,5-dimethylthiazol-2-yl)-2,5-diphenyltetrazolium bromide, M6494, Thermo Fischer Scientific) assay. Briefly, 10 μ l MTT solution (5mg/ml) was added to each well and incubated for 2 hours at 37°C. After incubation, the plates were centrifuged at 1200 rpm for 5 minutes at room temperature and the media was removed. The purple-colored formazan crystals were dissolved by adding 100 μ l DMSO (D5879, Sigma Aldrich) and the absorbance at 570 nm was measured using plate reader (Tecan)

2.5 Tumorsphere assay

For sphere assay, T1 and T2 cells were trypsinized and washed with DPBS. These cell populations were then resuspended in serum free DMEM/F-12 media supplemented with 1X B27 (17504-044, Thermo Fischer Scientific), 20ng/mL bFGF (GF003, Sigma Aldrich), 4 μ g/mL Heparin (H3149-50KU, Sigma Aldrich). Both the cells were seeded at a density of 1×10^3 cells per well in an ultra-low attachment 24 well plate (Corning, Sigma). Media was replenished every third day and the tumorspheres were counted by day 5.

2.6 Quantitative real time PCR (qRT-PCR)

Total RNA was isolated using Trizol[®] reagent (15596026, Thermo Fischer Scientific) and 1.5 μ g of RNA was used for cDNA preparation using the High-Capacity cDNA Reverse Transcription Kit (4374966, Thermo Fisher Scientific). Real-time PCR was performed using iTaq Univer SYBR Green (1725121,

BioRad) on the QuantStudio 7 Flex RealTime PCR System (Applied Biosystems). The PCR conditions are 95° C for 10 minutes, followed by 40 cycles of 95° C for 30 seconds, and 60° C for 1 minute. All reactions were performed in triplicates and the transcript levels are normalized to those of β -actin. The relative fold change is determined by $2^{-\Delta\Delta CT}$ method.

2.7 Hematoxylin & Eosin (H & E) staining

Breast tumor tissues from mice were placed on the sample cassettes and fixed in 10% neutral buffered Formalin (24-72 hours) and transferred into PBS. Samples were embedded in paraffin and 5 μ m thick sections were taken. Subsequently, the tissue sections were stained using Hematoxylin and Eosin (H &E) and examined for metastases. After incubating at 60° C for one hour, the sections were deparaffinized in Xylene followed by rehydration in graded isopropanol solutions. The slides were then rinsed in tap water and kept in acid alcohol for 3 seconds again followed by tap water wash. Subsequently, the slides were dipped in bluing solution three-four times. Afterwards, the slides were rinsed thrice with tap water and transferred into 70% isopropanol for 3 minutes. Following this, the sections were stained with Eosin Y for 10 minutes. After staining, dehydration was performed in graded isopropanol followed by clearing in Xylene. The slides were then mounted with DPX and were visualized using bright field microscope (Leica).

2.8 RNA sequencing

Total RNA from three replicates each of 4T1GFP (parental cell line), T1 and T2 cells were isolated using the RNeasy minikit (74104, Qiagen) according to manufacturer's instructions. RNA concentration of the samples was estimated using Qubit RNA Assay BR (Q10211, Invitrogen). RNA purity was determined using QIAxpert and RNA integrity was measured using RNA ScreenTapes (5067-5576, Agilent) on TapeStation. All the 9 RNA samples passed the QC and were used for the library prep. A modified Illumina TruSeq RNA Sample Preparation V2 protocol (RS1222001) was used for making RNA sequencing libraries. The initial RNA Concentration of 500 ng was taken. First, the total RNA sample was subjected to mRNA enrichment by using Poly(A) purification beads. After purification, the mRNA was fragmented under elevated temperatures using divalent cations followed by cDNA synthesis. Indexed adapters were ligated to the cDNA and was then purified and enriched using the following thermal conditions: initial denaturation 98°C for 30 seconds; 13 cycles of 98°C for 10 seconds, 60°C for 30 seconds, 72°C for 30 seconds; final extension of 72°C for 5minutes. PCR products were then purified and checked on TapeStation D1000 DNA tapes (5067-5582, Agilent) for fragment size distribution. Using Qubit High Sensitivity Assay (Q32852, Invitrogen), the prepared libraries were quantified. Before cluster amplification, the libraries were pooled and diluted to the final loading concentration. After completing the cluster generation, the flow cell was loaded on

Illumina HiSeqX instrument and 150bp paired end reads were generated.

2.9 Bioinformatic analysis

The FASTq files obtained after sequencing was checked for quality using FASTQC software. Following the quality check, the adapters were removed from the sequences using Trimmomatic tool. After trimming the adaptors and subsequent quality check, the reads were aligned to the mouse reference genome (Mm10) using TopHat2. HTSeq tool was used to obtain the read counts after alignment. The obtained read counts were normalized and differential gene expression analysis was performed using DESeq2. The genes which showed a false discovery rate (FDR) adjusted p value (q value) < 0.01 and Log2FC >2 were considered statistically significant. Heatmap of the differentially expressed genes were constructed using HeatMap tool in the GenePattern software.

2.10 Kaplan Meier plotter

The top 50 differentially regulated genes with q value < 0.01 and Log2FC >2 were filtered based on their prognostic significance in triple negative breast cancer (TNBC) patients. The association of candidate gene expression with the survival of TNBC patients were analyzed using Kaplan-Meier plotter (KM plotter) database (<http://kmpplot.com/analysis/>) which derives the gene expression and survival data of breast cancer patients from the gene expression omnibus (GEO) database. After entering the gene list in to the KM plotter database, the patient samples were split by auto-selecting best cut-off. The association of relapse free survival (RFS, n=152) and distant metastasis free survival (DMFS, n=137) with each candidate gene was determined. The analysis was performed on breast cancer patients with negative ER, PR and HER2 status). The hazard ratio (with confidence intervals) and p values were obtained from the KM plotter.

2.11 Analysis of single cell transcriptomic data of human breast cancer samples

The human breast cancer single-cell RNA-seq dataset previously reported by Wu et al. (37) was downloaded from the Broad Institutes Single Cell Portal (https://singlecell.broadinstitute.org/single_cell/study/SCP1039/a-single-cell-and-spatially-resolved-atlas-of-human-breast-cancers#study-download). For further information detailing pre-processing, clustering, and cell type annotation, please refer to the authors publication. The data was loaded into R and recompiled into a Seurat (v4) (38) object using the sourced matrix, feature, and barcode files. The Seurat object was sub-set to include only barcodes identified as “cancer epithelial” using the metadata provided by the authors; similarly, the UMAP embedding was recreated using UMAP coordinates obtained from the single cell portal. Only the TNBC clusters were used for further analysis. The TNBC clusters were

broadly stratified into three groups (low, med, high) based on the average expression of MACC1 and visualized using plotting methods implemented in various R packages. Since the authors reported cluster segregation being strongly driven by patient of origin, this binning procedure was also applied to cluster 4 in isolation. Cluster 4 was chosen due to high relative intratumoral heterogeneity alongside cells with high MACC1 expression. The statistical analyses described were executed on both the aggregated TNBC clusters and on cluster 4 alone, however, to minimize patient specific differences unrelated to MACC1 expression and ensure robust comparisons, a focus was put on cluster 4. Differentially expressed genes (DEGs) were identified using the MAST (39) statistical framework implemented in Seurat’s ‘FindMarkers’ method. The analysis was conducted on the high vs. low MACC1-expressing subpopulations of cluster 4. DEGs with an average log 2 fold change ≥ 0.5 and an adjusted p-value <0.05 were used as input to the R package “enrichR”, which provides an interface to the Enrichr database (40) A hypergeometric test was performed using enrichR to determine enrichment of Gene Ontology terms associated with the “GO_Biological_Process_2021”, “GO_Molecular_Function_2021”, and “GO_Cellular_Component_2021” databases (40, 41) Pathway enrichment was also evaluated using “The Kyoto Encyclopedia of Genes and Genomes” (KEGG) database (41). To assess gene co-expression, pairwise Pearson correlations were computed between MACC1 and every other expressed gene in cluster 4 using the ‘cor.test’ function implemented by the “Stats” R package. To counteract the impact of multiple comparisons, a Bonferroni correction was applied to each p-value. The same methods were repeated post removal of ribosomal genes.

2.12 siRNA mediated knockdown of Macc1

6×10^3 T1 cells were seeded in 96 well plates. For small interference RNA (siRNA) mediated knockdown of Macc1, T1 cells were reverse transfected with 50 nM of universal negative control (control) and targeting MISSION® Predesigned siRNA (Sigma Aldrich) using Lipofectamine 2000 following manufacturer’s instructions in optiMEM (31985062, Thermo Fisher Scientific) media. After 24 hours, media was changed with fresh DMEM/F-12 media. The cell proliferation 48 hours post transfection was analyzed by MTT assay. For RNA isolation, 2.5×10^5 T1 cells were seeded in a 6 well plate. 48 hours after transfection, RNA was isolated from the plates using Trizol method.

2.13 Lovastatin treatment

Lovastatin was obtained from Santacruz biology and was dissolved in dimethyl sulfoxide (DMSO). 10 mM stock of Lovastatin was stored at -20°C in aliquots to avoid repeated freeze thawing. To see the effect of Lovastatin on cell proliferation, 1×10^3 T1 cells were seeded in 96 well plate. After 24 hours, the cells were treated with increasing concentrations of Lovastatin (1, 2.5, 5, 7.5 and 10 μM). T1 cells treated with an

equal amount of solvent (DMSO) was used as the control. The cell proliferation 48 hours post Lovastatin treatment was analyzed by MTT assay. For RNA isolation, 5×10^5 T1 cells were seeded in 60 mm cell culture plates. After 24 hours, the cells were treated with 6 μ M Lovastatin. Total RNA was isolated from Control and Lovastatin treated cells using Trizol method 48 hours post Lovastatin treatment.

2.14 Western blotting

T1 and T2 cells were lysed and protein was isolated using Radioimmunoprecipitation assay (RIPA) lysis buffer (R0278-50ML, Sigma-Aldrich) with protease inhibitor (P8340-5ML, Sigma-Aldrich). The protein concentrations were quantified using BCA assay (23225, Thermo Fisher Scientific). 25 μ g of total protein lysate was loaded on to 10% SDS gel and western blotting was performed as previously described (42). Antibodies used in the study are listed in [Supplementary Table 5](#).

2.15 Statistical analysis

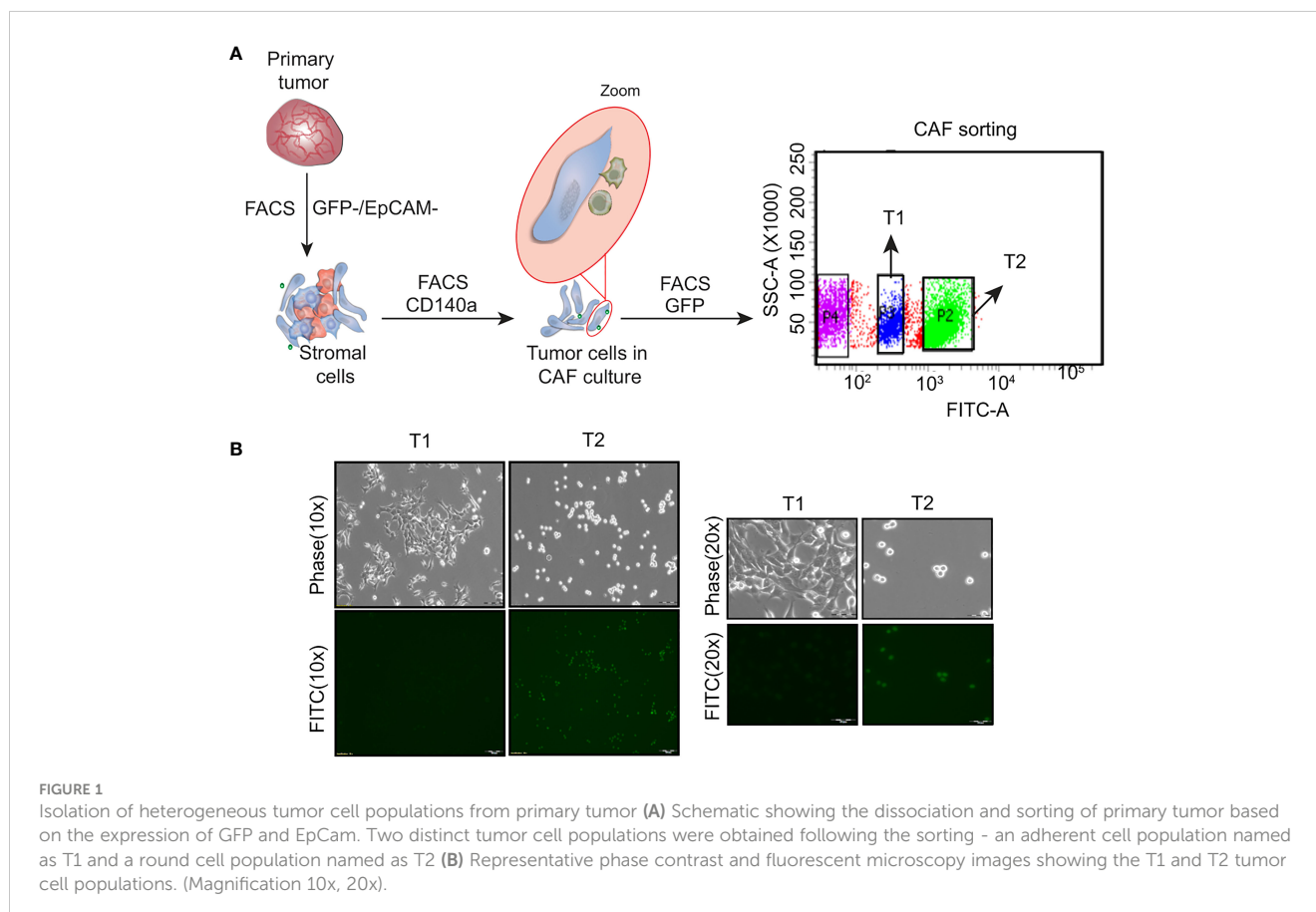
Statistical analyses were performed using GraphPad Prism 6 (GraphPad Software, Inc., San Diego, CA, USA). All experiments were performed in at least three biological replicates. Data are represented as mean \pm standard deviation. Statistical tests used are

un-paired Student's t-test and two-way ANOVA. p-values < 0.05 were considered statistically significant with * $p < 0.05$, ** $p < 0.01$, *** $p < 0.001$, **** $p < 0.0001$.

3 Results

3.1 Two distinct tumor cell populations were obtained from the primary tumor

Heterogeneous tumor cell populations were isolated from the 4T1GFP syngeneic tumor model as shown in [Supplementary Figure 1](#). The primary tumor was surgically resected 30 days post injection (when the tumor reached the ethical volume) to recapitulate the resection that patients undergo in a clinical setting. The primary tumor was then dissociated into single cells and sorted by flow cytometry into tumor epithelial (GFP+) and stromal fractions (GFP-) ([Figure 1A](#); [Supplementary Figure 2A](#)). The stromal population was further sorted based on the expression of CD140a to obtain cancer associated fibroblasts (CAFs) (GFP-/CD140a+) ([Supplementary Figure 2B](#)). However, we noticed the presence of few GFP+ tumor epithelial cells along with the fibroblast cells when the sorted CAF (GFP-) cells were cultured. As shown in [Supplementary Figure 2C](#), the GFP+ tumor epithelial cells eventually outnumbered the CAFs. We then resorted this CAF-tumor cell mixed population based on GFP expression to separate the GFP+ tumor epithelial cells ([Figure 1A](#)). Two tumor epithelial



cell populations that showed distinct GFP expression levels were obtained from the GFP+ fraction - a GFP^{High} (High GFP expression) and a GFP^{Low} (Low GFP expression) cell population. Interestingly, these cell populations also displayed different morphological appearance when cultured *in vitro* which was similar to observations made by Xiang and colleagues (Figure 1B) (14). The GFP^{High} cells showed a round and loosely adherent morphology whereas GFP^{Low} cell population exhibited adherent, 4T1 like morphology. These cells will be referred to as T1 (GFP^{Low}, Adherent) and T2 (GFP^{High}, Round) in the following sections.

3.2 *In vitro* characterization of T1 and T2 tumor cell populations

In vitro phenotypic characterization of the T1 and T2 tumor cell populations was performed to study the observed morphological heterogeneity at a functional level. Proliferation analysis using the MTT assay revealed that the T1 cells showed significantly higher proliferation rate compared to T2 cells (Figure 2A). We next looked at a key attribute of cancer cells, self-renewal ability and observed that the T2 cells showed significantly higher self-renewal ability compared to T1 cells as indicated by the number of primary tumorspheres (Figure 2B). The T1 and T2 tumor cells were also different in terms of the expression of epithelial markers (EpCam,

E-Cadherin), mesenchymal markers (Vimentin, Pdgfra) and dormancy associated marker (Nr2f1) as shown by the qRT-PCR analysis (Figure 2C).

3.3 Phenotypic heterogeneity is linked to distinct disease outcome

The results from the *in vitro* characterization showed that we had successfully isolated two distinct tumor cells from the bulk cancer mass. We next addressed the question if the *in vitro* phenotypic heterogeneity we observed, translated to different tumorigenic capacity *in vivo*. The T1 and T2 tumor cells were orthotopically injected into the mammary fat-pad of 6 to 8 week old BALB/c female mice and primary tumor growth was monitored over 30 days. Interestingly, all the mice (5/5) that were injected with the T1 tumor cells formed primary tumors. In contrast, only 2 out of the 9 mice injected with the T2 cells formed tumors that were significantly smaller than the T1 tumors (Figures 3A, B). This fits in well with our observation that T1 tumor cells showed higher proliferation rate *in vitro* when compared to T2 cells. We next performed the Kaplan Meier survival analysis on the mice injected with T1 and T2 tumor cells (Figure 3C). Mice injected with the T1 tumor cells showed a median survival of 31 days whereas the mice injected with T2 cells showed a median survival of 150 days. Log-

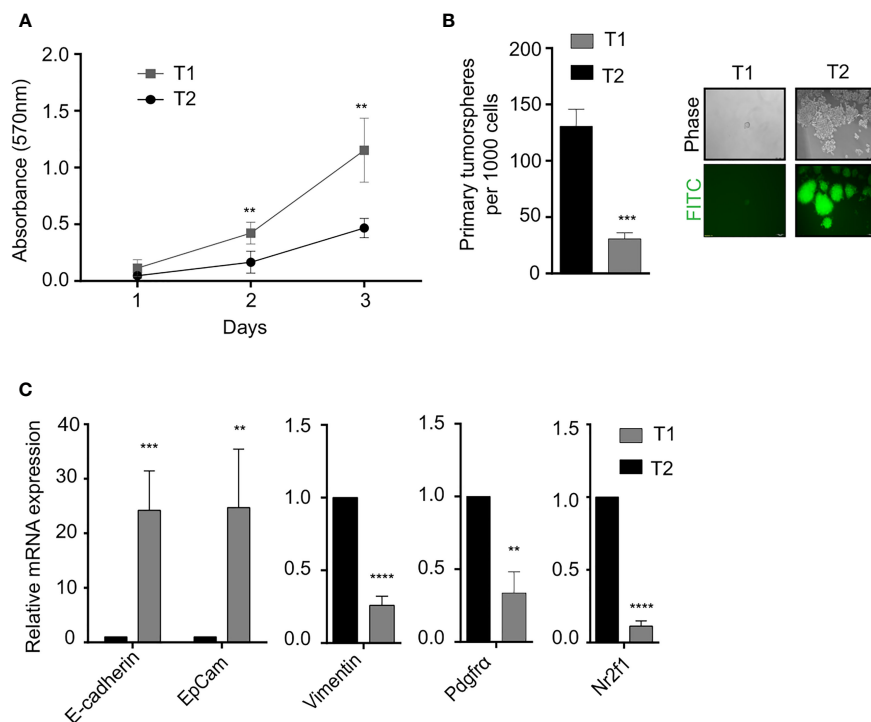


FIGURE 2

Phenotypic characterization of T1 and T2 tumor populations from primary tumor (A) Proliferation analysis using MTT assay shows that T1 cells proliferated at a significantly faster rate. (B) Quantification of the number of primary tumorspheres formed by the T1 and T2 populations in tumor-sphere assay. Phase contrast and fluorescence microscopy images showed that T1 cells formed fewer and smaller tumorspheres (C) Quantitative real-time PCR showing the relative mRNA expression of epithelial-mesenchymal and quiescence genes in the T1 and T2 populations from the primary tumor. Data are expressed as mean \pm standard deviation. $n=3$, $p < 0.05$ are considered statistically significant with $**p < 0.01$, $***p < 0.001$, $****p < 0.0001$.

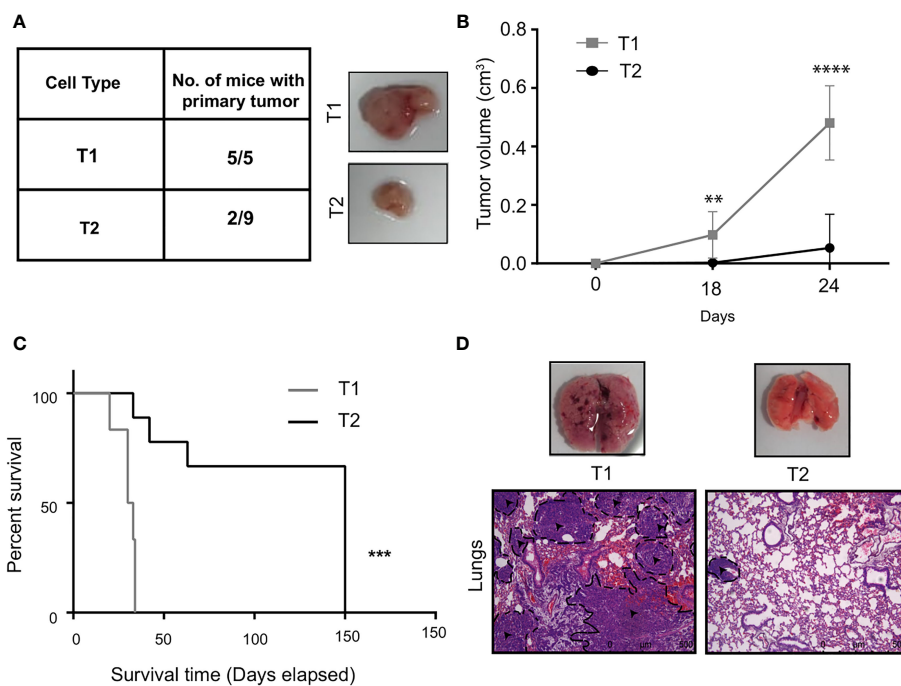


FIGURE 3

T1 cells showed highly aggressive disease outcome (A) *In vivo* tumorigenic potential of T1 and T2 tumor cells were analyzed by injecting 7×10^5 tumor cells orthotopically into the fourth mammary fat-pad of BALB/c mice. Table shows the number of mice that developed primary tumors/ number of mice injected. Representative image shows the primary tumors formed by T1 and T2 tumor cells after 4 weeks. The T1 cells are highly aggressive as they formed larger primary tumors compared to the T2 cells (B) Tumor growth curves of mice injected with T1 (n=5) and T2 cells (n=9) (C) Percentage survival of mice injected with T1 and T2 tumor cells. (D) Representative H&E staining of lungs of mice injected with 5×10^5 T1 and T2 tumor cells via the lateral tail veins (n=5). The black dashed lines and arrows indicating the metastatic lesions. Magnification 10x. ** $p < 0.01$, *** $p < 0.001$, **** $p < 0.0001$.

rank test revealed that mice injected with T1 tumor cells had significantly lower survival rate compared to mice injected with the T2 tumor cells ($p = 0.0004$). We also analyzed the metastatic potential of these two cell types using the experimental metastasis assay. We injected the T1 and T2 tumor cells via the lateral tail vein of BALB/c mice (n=5 each). After sacrificing the mice, lungs were harvested and examined for metastases. As shown by the representative H&E staining, all the mice injected with the T1 cells formed large lung macrometastases (5/5) (Figure 3D). The mice injected with the T2 cells did not exhibit lung metastasis in all the samples (4/5) and the metastases formed were smaller in size (average number of metastases per mouse = 6.4, Supplementary Table 1). The highly proliferative T1 cells formed large macrometastases in all the mice (5/5) and could not be quantified. The *in vivo* results clearly showed that the T1 tumor cells have significantly higher tumorigenicity and metastatic potential compared to the T2 cells (Supplementary Table 2).

3.4 Identification of candidate genes associated with poor prognosis of TNBC patients

To identify the differentially expressed genes involved in mediating the phenotypic heterogeneity in the 4T1 primary tumor

and aggressive phenotype of T1 cells compared to the T2 cells, we performed transcriptomic analysis on the 4T1GFP (parental), T1 and T2 cells using RNA sequencing (Supplementary Figure 3). RNA sequencing was performed using the Illumina HiSeqX platform. The read counts were normalized and differential gene expression analysis was performed using DESeq2 which uses median of ratios as normalization method. The top candidate genes were then identified based on the filters such as $q\text{-value} < 0.01$ and Log_2 fold change > 2 (Supplementary Figure 3). Based on the filters, top 50 candidate genes upregulated in the T1 compared to T2 population were obtained (Supplementary Table 3).

In order to identify the genes contributing to the aggressive disease phenotype in the T1 cell population, we analyzed the association of the top 50 candidate gene's expression with relapse and distant metastasis free survival (RFS and DMFS) in breast cancer using publicly available curated clinical datasets like TCGA in the Kaplan Meier (KM) plotter software. Macc1 was identified as the top gene for further validation as TNBC patients with a higher mean expression of MACC1 showed poor relapse-free survival (RFS - Hazards ratio/HR: 2.38, log p value: 0.01) and distant metastasis-free survival (DMFS, HR: 2.21, log p value: 0.019) compared to the patients with lower MACC1 expression (Figures 4A, B). We have analyzed the expression of Macc1 at protein level in the T1 and T2 cells. T1 cells showed significantly higher expression of Macc1 compared to T2 cells (Supplementary Figure 5B) validating our RNA sequencing analysis.

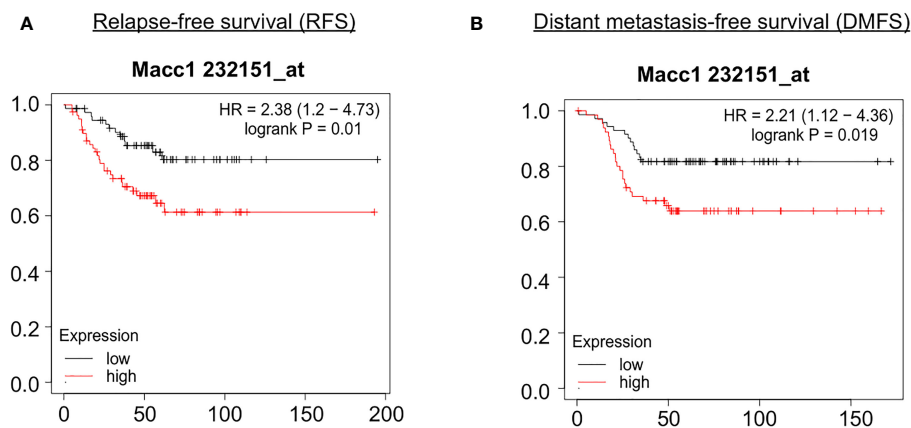


FIGURE 4

Association of relapse and distant metastasis-free survival of TNBC patients with expression of MACC1. Correlation of MACC1 gene expression with TNBC patient survival was analyzed using KM plotter. TNBC patients with higher expression (red line) of MACC1 was associated with significant lower relapse-free survival (A) and distant metastasis-free survival (B) compared to the patients with lower expression of MACC1 (black line).

3.5 Investigating the correlation of higher MACC1 expression with aggressive disease phenotype in human TNBC patients at single cell level

We next took the important step of correlating differential MACC1 expression with disease phenotype in human patient samples. We analyzed previously published single cell RNA sequencing data (37) and stratified the malignant epithelial cells based on molecular subtypes. We only retained the TNBC annotated clusters using the UMAP coordinates which resulted in 7 clusters with each cluster representing a single tumor/patient sample (Figure 5A). We screened each TNBC cluster for MACC1 expression using gene-weighted density estimation based on the log normalized counts of each cell (Figure 5B). In order to minimize potential noise from patient-specific differences, we focused on only one cluster - cluster 4, as it showed highest overall Macc1 expression. Interestingly, cluster 4 also displayed higher intratumoral heterogeneity within the malignant individual cells leading to a clear bifurcation in the cluster (Figure 5B). In order to investigate the intratumoral heterogeneity in the MACC1 expression in cluster 4 (Figure 5C), we binned the cells based on their average MACC1 expression. We collapsed the medium and high expression groups into a single group to improve the power of our comparisons though it reduced the magnitude of the average expression value of MACC1 between the groups being compared (low MACC1 expressing cells = 189 and medium/high MACC1 expressing cells = 94). Interestingly, a clear distinction in the gene expression pattern of cluster 4 was observed (Figure 5C). To identify the genes and pathways associated with higher MACC1 expression, we looked at the genes that are differentially regulated in the MACC1 high versus low cells in cluster 4 (Figure 5C). Cells assigned to the high MACC1 expression bin were found to be enriched in genes associated with the gene ontology (GO) term 'positive regulation of angiogenesis' (data not shown). This is interesting as MACC1 has already been reported to promote

angiogenesis in many cancers (43). In addition, we also performed the analysis of the pair wise gene correlation based on Pearson's correlation coefficient and identified the top 12 genes that showed significant positive correlation with MACC1 expression (Figure 5D). The functional relevance of these genes in breast cancer progression was then determined. Among the positively correlated genes, EF1A1, TPT1, S100A11, PABPC1, B2M, CLDN4, HSP90AA1, UQCRH were found to be associated with aggressive disease phenotype in breast cancer (44–50). For example, EF1A1 (Eukaryotic translation elongation factors 1 alpha 1), is known to promote tumor cell proliferation, migration and invasion in TNBC cells. Our results point to the molecular mechanism by which MACC1 can contribute to the aggressive disease phenotype in human TNBC which is being explored further in future work.

3.6 Macc1 depletion caused significant reduction in breast cancer cell proliferation

Macc1 is known to regulate a number of cellular functions in cancer including cell proliferation. We performed siRNA-based silencing of Macc1 in the aggressive T1 cells in order to evaluate the role of Macc1 gene expression in breast cancer cell proliferation. We first looked at the mRNA levels to determine if the knock down had worked. A significant reduction in the expression of Macc1 was observed 48 hours post-transfection (Figure 6A). Interestingly, Macc1 silencing resulted in significantly lower cell viability (Figure 6B) in the knock down tumor cells (siMacc1) compared to T1 tumor cells (Control).

We were interested in extending this finding to a clinical context by using Lovastatin, a small molecule transcriptional inhibitor of Macc1 (51, 52). T1 cells were treated with increasing concentrations of Lovastatin for 48 hours (Figure 6C). Treatment with Lovastatin resulted in a significant decrease in the T1 cell proliferation in a dose dependent manner (Figure 6C). We further analyzed the effect of

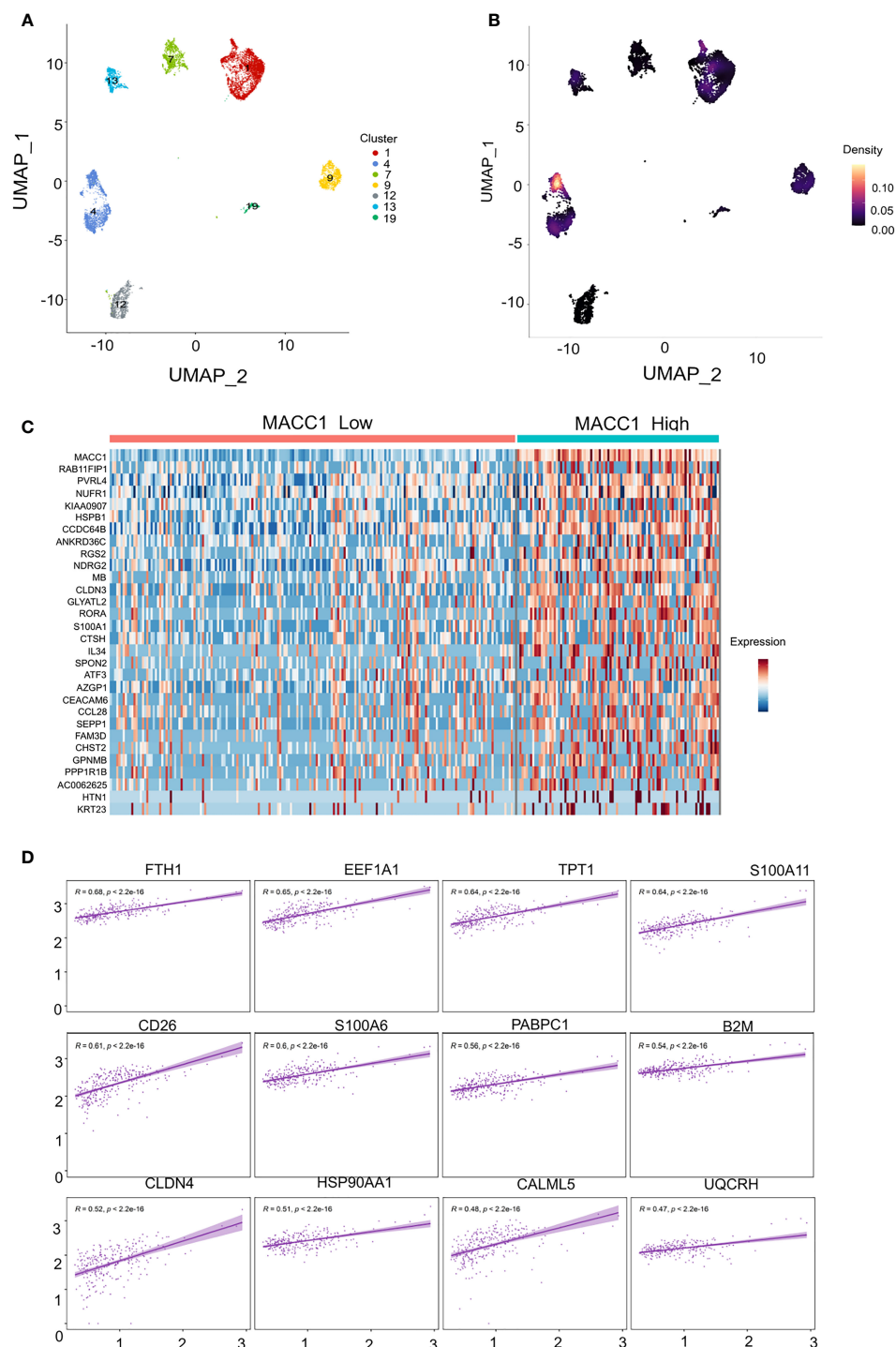


FIGURE 5 Single cell transcriptomic analysis of MACC1 expression in human TNBC samples (A) UMAP visualization of all malignant epithelial cells in the human TNBC samples (n= 7) (B) Density UMAP visualization of MACC1 expression in each of the TNBC samples (Yellow color showing highest MACC1 expression and black showing the least. (C) Heatmap showing top 15 up and down regulated genes associated with MACC1 high versus low cells (D) Top 12 positively correlated genes associated with MACC1 expression in cluster 4 (after excluding the ribosomal genes).

Lovastatin on Macc1 expression. The expression of Macc1 mRNA was significantly diminished after Lovastatin treatment (Figure 6D). This result demonstrates proof of principle that we can target the T1 aggressive cells within a heterogenous tumor mass effectively via Macc1, by using the small molecule inhibitor Lovastatin.

4 Discussion

Breast cancer manifests itself in different clinico-pathological forms depending on underlying gene signatures. Intertumoral heterogeneity has been at the heart of treatment modalities of

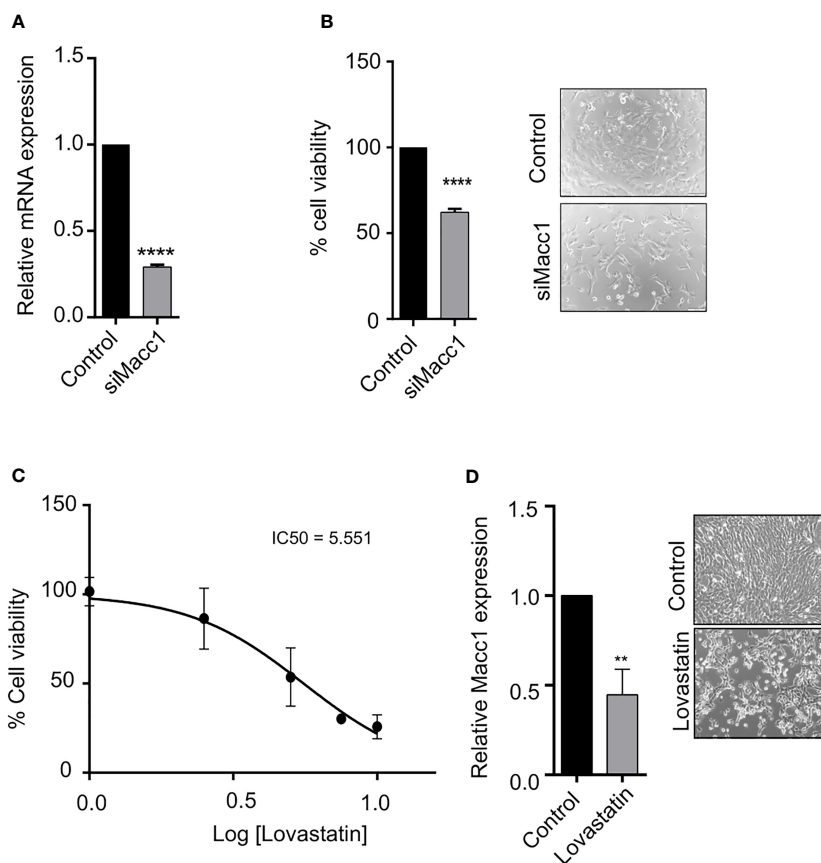


FIGURE 6

Targeting Macc1 expression affected the proliferation of aggressive breast cancer cells (A) Relative expression of Macc1 mRNA in T1 cells transfected with Macc1 siRNA compared to the control as quantified by the qRT-PCR. (B) Percentage cell viability of T1 cells following transfection of control and Macc1 siRNAs. The cells were reverse transfected with 50nM siRNAs and the cell proliferation after 48 hours were analyzed using MTT assay. Knockdown of Macc1 caused a significant reduction in the percentage cell viability compared to control. Phase contrast microscopy images showing the T1 cells transfected with Macc1 siRNA compared to control cells are shown as inset. (C) Graph showing the percentage cell viability of T1 cells after Lovastatin treatment. T1 cells were treated with different concentrations of Lovastatin (1, 2.5, 5, 7.5 and 10 μ M) and cell viability after 48 hours was measured using MTT assay. The IC₅₀ concentration of Lovastatin for T1 cells was then calculated using GraphPad Prism software. (D) The relative mRNA expression of Macc1 in Lovastatin (6 μ M) treated cells compared to control as analyzed by qRT-PCR. Macc1 expression was normalized to β -actin. Phase contrast microscopy images showing the T1 cells treated with Lovastatin (6 μ M) compared to DMSO treated (control) cells are shown as inset. $n=3$, $p < 0.05$ are considered statistically significant with $**p < 0.01$, $****p < 0.0001$.

breast cancer with the success in breast cancer management arising largely from the use of targeted therapy like Tamoxifen in ER+ and Herceptin for the Her2 subtypes. But the increasing spotlight on the different cell types within a single tumor termed intratumoral heterogeneity results in the challenging situation where drug resistant cells escape and lead to relapse of the tumor. This is particularly true in the TNBC molecular subtype which though classified as a single entity based on immuno-histochemistry (IHC), actually is a group of diseases. More recent work has shown that there could also be unique “ecotypes” within tumors involving the interaction of cancer cells with the microenvironment (37) thus complicating the picture. Our work aims to deconvolute the different cell populations within a single TNBC tumor and understand if we could exploit the underlying molecular circuitry for therapeutic purposes.

The 4T1 model had previously been reported to have morphologically distinct cell types by Xiang et al., although they did not isolate and study the relationship of morphologically

distinct tumor cells with disease outcomes due to technical challenges (35). We overcame this hurdle by tagging the heterogenous bulk cell population with a GFP tag, which enabled us to isolate multiple tumor cells based on their GFP expression and culture them *in vitro*. We decided to focus our current work on two cell types that displayed striking morphological distinctness in multiple passages *in vitro*. More importantly, the morphological difference also translated into differing growth kinetics, self-renewal capacity, EMT molecular markers and contrasting disease outcomes *in vivo*. This confirmed our hypothesis that a tumor is composed of non-identical cells which coexist to give different functionality to the cancer (33). We hypothesized that the slow cycling T2 cells are more stem-like when compared to T1 cells. We observed a significantly higher self-renewal ability in T2 cells in the tumorsphere assay (Figure 2B). In addition, T2 cells have higher expression of a dormancy associated marker Nr2f1 (4, 5) (Figure 2C) pointing towards their quiescent nature. In order to further test the *in vivo* self-renewal and tumor propagating capacity

of the T1 and T2 cells, we will perform *in vivo* long-term tumor growth assays as a part of our future study.

In addition to this, we analyzed the EMT scores of the three cell populations by applying three different scoring methods – a 76 gene EMT signature (76GS), Kolmogorov Smirnov (KS) method and Multinomial logistic regression (MLR) method (Chakraborty et al., 2020) using the global gene expression data, to determine the epithelial-mesenchymal status of the cells. Interestingly, the EMT score calculation by all the three methods showed that the T2 cells are more mesenchymal than the 4T1GFP parental and T1 cells which aligns with our *in vitro* findings (Supplementary Figure 4, Supplementary Table 4). We have also analyzed the expression of E-Cadherin and Vimentin at protein level. We observed a high expression of E-Cadherin in the T1 cells however there was no significant change in the expression of Vimentin between T1 and T2 cells (Supplementary Figure 5A).

The molecular mechanism of Macc1 has been extensively investigated in colorectal cancer. Macc1 is the transcriptional activator of MET and triggers the downstream PI3K-AKT and MEK/ERK signaling pathway (53). We are currently in the process of investigating the molecular pathways perturbed in the TNBC on treatment with Lovastatin that is outside the purview of the current manuscript. Our work also underscores the critical need to target different pools of tumor cells in order to get long term clinical benefit. As proof of principle for a therapeutic approach to target the aggressive T1 tumor cells, we identified Macc1 as a key gene over expressed in T1 cells and involved in the proliferative phenotype. We went on to test the therapeutic relevance of Lovastatin, as a potential candidate for treatment of TNBC patients. Lovastatin belongs to a class of a cholesterol lowering drugs called “Statins” that are widely used in treating chronic cardiovascular conditions like hypercholesterolemia (54). Lovastatin targets the rate-limiting step of the biosynthetic mevalonate pathway by inhibiting HMG-CoA reductase, thereby lowering the cholesterol levels (51). In addition to Lovastatin, several other statins including Fulvastatin, Atorvastatin, Simvastatin and Pitavastatin have also been found to reduce Macc1 expression in multiple cancer cell lines including colorectal, gastric and pancreatic cancer (55). Crucial to our hypothesis, we found that Lovastatin did cause a significant decrease in the viability of the T1 tumor cells. This is an important step in repurposing a class of drugs to target different populations in a cancer by targeting molecules critical to different cell types.

Targeting a single subpopulation of tumor cells may not be sufficient to debulk the entire tumor. Interestingly, the 4T1GFP parental cells displayed similar proliferation and tumor growth kinetics as that of the T1 cells. The correlation heatmap of the transcriptomic analysis showed that the gene expression of 4T1GFP parental cells is similar to that of T1 cells (Supplementary Figures 6A, B, C). In contrast, the 4T1GFP parental cells showed significantly lower sensitivity to Lovastatin treatment compared to T1 cells (IC50 10.96 μ M and 5.551 μ M respectively) (Supplementary Figure 6D) pointing to the existence of different cell populations contributing to heterogeneous therapeutic response. In addition, the different cell types within the tumor can engage in cooperation and competition

which could further influence the response to therapy (56). It will be important to understand how these cells interact with each other and collectively impact the tumor growth and therapeutic response in future work.

Our work thus adds to the growing understanding of the contribution of different cell types to tumor growth and drug response. The ability to identify and then effectively eliminate these distinct populations within a tumor will be key to achieve long term, sustained therapeutic response and better patient prognosis in TNBC.

Data availability statement

The datasets presented in this study can be found in online repositories. The names of the repository/repositories and accession number(s) can be found in the article/Supplementary Material. The datasets generated in this study can be found under the GEO accession number GSE195995.

Ethics statement

All animal experiments were carried out according to the regulations of the Institutional Animal Ethics Committee (IAEC), RGCB.

Author contributions

Conceptualization, RN and AT; methodology, AT, SR, RM, PC, NK, BV, VJ, MJ, SR, AS, and RN; validation, AT; formal analysis, AT, SRT, RM, PC, NK, BV, VJ, and SR; investigation, RN; resources, RN; writing—original draft preparation, AT and RN; writing—review and editing, all authors; visualization, AT and NK; supervision, RN; project administration, RN; funding acquisition, MJ and RN. All authors contributed to the article and approved the submitted version.

Funding

RN is the recipient of the Ramanujan Fellowship from the Government of India (SERB) (SB/S2/RJN/182/2014) and intramural funding from Rajiv Gandhi Centre for Biotechnology, Kerala, India. MJ was supported by Ramanujan Fellowship (SB/S2/RJN-049/2018) provided by SERB, DST, Government of India, and by InfoSys Foundation, Bangalore. AT was supported by CSIR senior research fellowship and SR was supported by fellowship from University Grants Commission (UGC), Government of India.

Acknowledgments

We thank RGCB for intramural funding. We thank Surabhi S.V. and Tilak Prasad for helping with flow cytometry, Nanditha C.K.

for helping with the histopathology, Aswathy Mary Paul and Bijesh George for helping with the computational analysis, Dr. Umashanker P.K. for sharing the reagents. This research was published in the preprints.org (36) and is a part of the thesis submitted for Manipal Academy of Higher Education (57).

Conflict of interest

The authors declare that the research was conducted in the absence of any commercial or financial relationships that could be construed as a potential conflict of interest.

References

- Turashvili G, Brogi E. Tumor heterogeneity in breast cancer. *Front Med* (2017) 4:227. doi: 10.3389/fmed.2017.00227
- Beca F, Polyak K. Intratumor heterogeneity in breast cancer. *Adv Exp Med Biol* (2016) 882:169–89. doi: 10.1007/978-3-319-22909-6_7
- Yin L, Duan JJ, Bian XW, Yu SC. Triple-negative breast cancer molecular subtyping and treatment progress. *Breast Cancer Res BCR* (2020) 22(1):61. doi: 10.1186/s13058-020-01296-5
- Dai X, Cheng H, Bai Z, Li J. Breast cancer cell line classification and its relevance with breast tumor subtyping. *J Cancer* (2017) 8(16):3131–41. doi: 10.7150/jca.18457
- Yam C, Mani SA, Moulder SL. Targeting the molecular subtypes of triple negative breast cancer: Understanding the diversity to progress the field. *Oncologist* (2017) 22(9):1086–93. doi: 10.1634/theoncologist.2017-0095
- Sharma P. Biology and management of patients with triple-negative breast cancer. *Oncologist* (2016) 21(9):1050–62. doi: 10.1634/theoncologist.2016-0067
- Li Y, Zhang H, Merkhher Y, Chen L, Liu N, Leonov S, et al. Recent advances in therapeutic strategies for triple-negative breast cancer. *J Hematol Oncol* (2022) 15(1):121. doi: 10.1186/s13045-022-01341-0
- Kumar P, Aggarwal R. An overview of triple-negative breast cancer. *Arch Gynecology Obstetrics* (2016) 293(2):247–69. doi: 10.1007/s00404-015-3859-y
- Kim C, Gao R, Sei E, Brandt R, Hartman J, Hatschek T, et al. Chemoresistance evolution in triple-negative breast cancer delineated by single-cell sequencing. *Cell* (2018) 173(4):879–93 e13. doi: 10.1016/j.cell.2018.03.041
- Borri F, Granaglia A. Pathology of triple negative breast cancer. *Semin Cancer Biol* (2021) 72:136–45. doi: 10.1016/j.semcancer.2020.06.005
- Norman Fultang MC, Bela Peethambaran Regulation of cancer stem cells in triple negative breast cancer. *Cancer Drug Resistance* (2021) 4:321–41. doi: 10.20517/cdr.2020.106
- Derakhshan F, Reis-Filho JS. Pathogenesis of triple-negative breast cancer. *Annu Rev Pathology* (2022) 17:181–204. doi: 10.1146/annurev-pathol-042420-093238
- Luond F, Tiede S, Christofori G. Breast cancer as an example of tumour heterogeneity and tumour cell plasticity during Malignant progression. *Br J Cancer* (2021) 125(2):164–75. doi: 10.1038/s41416-021-01328-7
- Xu Q, Kaur J, Wylie D, Mittal K, Li H, KolaChina R, et al. A case series exploration of multi-regional expression heterogeneity in triple-negative breast cancer patients. *Int J Mol Sci* (2022) 23(21). doi: 10.3390/ijms232113322
- Wright N, Rida PCG, Aneja R. Tackling intra- and inter-tumor heterogeneity to combat triple negative breast cancer. *Front Bioscience* (2017) 22(9):1549–80. doi: 10.2741/4558
- Kvokackova B, Fedr R, Kuzilkova D, Stuchly J, Vavrova A, Navratil J, et al. Single-cell protein profiling defines cell populations associated with triple-negative breast cancer aggressiveness. *Mol Oncol* (2023) 17(6):1024–40. doi: 10.1002/1878-0261.13365
- Karaayvaz M, Cristea S, Gillespie SM, Patel AP, Mylvaganam R, Luo CC, et al. Unravelling subclonal heterogeneity and aggressive disease states in TNBC through single-cell RNA-seq. *Nat Commun* (2018) 9(1):3588. doi: 10.1038/s41467-018-06052-0
- Zhou S, Huang YE, Liu H, Zhou X, Yuan M, Hou F, et al. Single-cell RNA-seq dissects the intratumoral heterogeneity of triple-negative breast cancer based on gene regulatory networks. *Mol Ther Nucleic Acids* (2021) 23:682–90. doi: 10.1016/j.omtn.2020.12.018
- Chiu AM, Mitra M, Boymoushakian L, Coller HA. Integrative analysis of the inter-tumoral heterogeneity of triple-negative breast cancer. *Sci Rep* (2018) 8(1):11807. doi: 10.1038/s41598-018-29992-5
- Bianchini G, De Angelis C, Licata L, Gianni L. Treatment landscape of triple-negative breast cancer - expanded options, evolving needs. *Nat Rev Clin Oncol* (2022) 19(2):91–113. doi: 10.1038/s41571-021-00565-2
- Marra A, Trapani D, Viale G, Criscitiello C, Curigliano G. Practical classification of triple-negative breast cancer: intratumoral heterogeneity, mechanisms of drug resistance, and novel therapies. *NPJ Breast Cancer* (2020) 6:54. doi: 10.1038/s41523-020-00197-2
- Hossain F, Majumder S, David J, Miele L. Precision medicine and triple-negative breast cancer: Current landscape and future directions. *Cancers* (2021) 13(15). doi: 10.3390/cancers13153739
- Lehmann BD, Jovanovic B, Chen X, Estrada MV, Johnson KN, Shyr Y, et al. Refinement of triple-negative breast cancer molecular subtypes: Implications for neoadjuvant chemotherapy selection. *PLoS One* (2016) 11(6):e0157368. doi: 10.1371/journal.pone.0157368
- Garrido-Castro AC, Lin NU, Polyak K. Insights into molecular classifications of triple-negative breast cancer: Improving patient selection for treatment. *Cancer Discovery* (2019) 9(2):176–98. doi: 10.1158/2159-8290.CD-18-1177
- Ramon YCS, Sese M, Capdevila C, Aasen T, De Mattos-Arruda L, Diaz-Cano SJ, et al. Clinical implications of intratumor heterogeneity: challenges and opportunities. *J Mol Med* (2020) 98(2):161–77. doi: 10.1007/s00109-020-01874-2
- Januskeviciene I, Petrikaite V. Heterogeneity of breast cancer: The importance of interaction between different tumor cell populations. *Life Sci* (2019) 239:117009. doi: 10.1016/j.lfs.2019.117009
- Minn AJ, Kang Y, Serganova I, Gupta GP, Giri DD, Doubrovina M, et al. Distinct organ-specific metastatic potential of individual breast cancer cells and primary tumors. *J Clin Invest* (2005) 115(1):44–55. doi: 10.1172/JCI22320
- Saeki S, Kumegawa K, Takahashi Y, Yang L, Osako T, Yasen M, et al. Transcriptomic intratumor heterogeneity of breast cancer patient-derived organoids may reflect the unique biological features of the tumor of origin. *Breast Cancer Res BCR* (2023) 25(1):21. doi: 10.1186/s13058-023-01617-4
- Wagenblast E, Soto M, Gutierrez-Angel S, Hartl CA, Gable AL, Maceli AR, et al. A model of breast cancer heterogeneity reveals vascular mimicry as a driver of metastasis. *Nature* (2015) 520(7547):358–62. doi: 10.1038/nature14403
- Jiang K, Dong M, Li C, Sheng J. Unraveling heterogeneity of tumor cells and microenvironment and its clinical implications for triple negative breast cancer. *Front Oncol* (2021) 11:557477. doi: 10.3389/fonc.2021.557477
- Marusyk A, Tabassum DP, Altmann PM, Almendro V, Michor F, Polyak K. Non-cell-autonomous driving of tumour growth supports sub-clonal heterogeneity. *Nature* (2014) 514(7520):54–8. doi: 10.1038/nature13556
- Janiszewska M, Tabassum DP, Castano Z, Cristea S, Yamamoto KN, Kingston NL, et al. Subclonal cooperation drives metastasis by modulating local and systemic immune microenvironments. *Nat Cell Biol* (2019) 21(7):879–88. doi: 10.1038/s41556-019-0346-x
- Martin-Pardillos A, Valls Chiva A, Bande Vargas G, Hurtado Blanco P, Pineiro Cid R, Guijarro PJ, et al. The role of clonal communication and heterogeneity in breast cancer. *BMC Cancer* (2019) 19(1):666. doi: 10.1186/s12885-019-5883-y
- Kuiken HJ, Dhakal S, Selfors LM, Friend CM, Zhang T, Callari M, et al. Clonal populations of a human TNBC model display significant functional heterogeneity and divergent growth dynamics in distinct contexts. *Oncogene* (2022) 41(1):112–24. doi: 10.1038/s41388-021-02075-y
- Xiang X, Zhuang X, Ju S, Zhang S, Jiang H, Mu J, et al. miR-155 promotes macroscopic tumor formation yet inhibits tumor dissemination from mammary fat

Publisher's note

All claims expressed in this article are solely those of the authors and do not necessarily represent those of their affiliated organizations, or those of the publisher, the editors and the reviewers. Any product that may be evaluated in this article, or claim that may be made by its manufacturer, is not guaranteed or endorsed by the publisher.

Supplementary material

The Supplementary Material for this article can be found online at: <https://www.frontiersin.org/articles/10.3389/fonc.2023.1230647/full#supplementary-material>

- pads to the lung by preventing EMT. *Oncogene* (2011) 30(31):3440–53. doi: 10.1038/onc.2011.54
36. Archana P, Thankamony SR, Murali R, Chakraborty P, Karthikeyan N, Varghese BA, et al. Phenotypic heterogeneity drives differential disease outcome in triple negative breast cancer. *Preprints.org* (2022). doi: 10.20944/preprints202202.0133.v1
37. Wu SZ, Al-Eryani G, Roden DL, Junankar S, Harvey K, Andersson A, et al. A single-cell and spatially resolved atlas of human breast cancers. *Nat Genet* (2021) 53(9):1334–47. doi: 10.1038/s41588-021-00911-1
38. Hao Y, Hao S, Andersen-Nissen E, Mauck WM 3rd, Zheng S, Butler A, et al. Integrated analysis of multimodal single-cell data. *Cell* (2021) 184(13):3573–87 e29. doi: 10.1016/j.cell.2021.04.048
39. Finak G, McDavid A, Yajima M, Deng J, Gersuk V, Shalek AK, et al. MAST: a flexible statistical framework for assessing transcriptional changes and characterizing heterogeneity in single-cell RNA sequencing data. *Genome Biol* (2015) 16:278. doi: 10.1186/s13059-015-0844-5
40. Kuleshov MV, Jones MR, Rouillard AD, Fernandez NF, Duan Q, Wang Z, et al. Enrichr: a comprehensive gene set enrichment analysis web server 2016 update. *Nucleic Acids Res* (2016) 44(W1):W90–7. doi: 10.1093/nar/gkw377
41. Gene Ontology C. The Gene Ontology resource: enriching a Gold mine. *Nucleic Acids Res* (2021) 49(D1):D325–D34. doi: 10.1093/nar/gkaa1113
42. Thankamony AP, Murali R, Karthikeyan N, Varghese BA, Teo WS, McFarland A, et al. Targeting the Id1-Kif11 axis in triple-negative breast cancer using combination therapy. *Biomolecules* (2020) 10(9). doi: 10.3390/biom10091295
43. Peng T, Li Z, Li D, Wang S. MACC1 promotes angiogenesis in cholangiocarcinoma by upregulating VEGFA. *OncoTargets Ther* (2019) 12:1893–903. doi: 10.2147/OTT.S197319
44. Luo Y, Kishi S, Sasaki T, Ohmori H, Fujiwara-Tani R, Mori S, et al. Targeting claudin-4 enhances chemosensitivity in breast cancer. *Cancer Science* (2020) 111(5):1840–50. doi: 10.1111/cas.14361
45. Neuhauser K, Kuper L, Christiansen H, Bogdanova N. Assessment of the role of translationally controlled tumor protein 1 (TPT1/TCTP) in breast cancer susceptibility and ATM signaling. *Clin Trans Radiat Oncol* (2019) 15:99–107. doi: 10.1016/j.ctro.2019.01.006
46. Pecorari L, Marin O, Silvestri C, Candini O, Rossi E, Guerzoni C, et al. Elongation Factor 1 alpha interacts with phospho-Akt in breast cancer cells and regulates their proliferation, survival and motility. *Mol Cancer* (2009) 8:58. doi: 10.1186/1476-4598-8-58
47. McKiernan E, McDermott EW, Evoy D, Crown J, Duffy MJ. The role of S100 genes in breast cancer progression. *Tumour Biol J Int Soc Oncodevelopmental Biol Med* (2011) 32(3):441–50. doi: 10.1007/s13277-010-0137-2
48. Cheng Q, Chang JT, Geradts J, Neckers LM, Haystead T, Spector NL, et al. Amplification and high-level expression of heat shock protein 90 marks aggressive phenotypes of human epidermal growth factor receptor 2 negative breast cancer. *Breast Cancer Res BCR* (2012) 14(2):R62. doi: 10.1186/bcr3168
49. Dong H, Wang W, Mo S, Liu Q, Chen X, Chen R, et al. Long non-coding RNA SNHG14 induces trastuzumab resistance of breast cancer via regulating PABPC1 expression through H3K27 acetylation. *J Cell Mol Med* (2018) 22(10):4935–47. doi: 10.1111/jcmm.13758
50. Owens KM, Kulawiec M, Desouki MM, Vanniarajan A, Singh KK. Impaired OXPPOS complex III in breast cancer. *PLoS One* (2011) 6(8):e23846. doi: 10.1371/journal.pone.0023846
51. Juneja M, Kobelt D, Walther W, Voss C, Smith J, Specker E, et al. Statin and rottlerin small-molecule inhibitors restrict colon cancer progression and metastasis via MACC1. *PLoS Biol* (2017) 15(6):e2000784. doi: 10.1371/journal.pbio.2000784
52. Dahlmann M, Werner R, Kortum B, Kobelt D, Walther W, Stein U. Restoring treatment response in colorectal cancer cells by targeting MACC1-dependent ABCB1 expression in combination therapy. *Front Oncol* (2020) 10:599. doi: 10.3389/fonc.2020.00599
53. Stein U, Walther W, Arlt F, Schwabe H, Smith J, Fichtner I, et al. MACC1, a newly identified key regulator of HGF-MET signaling, predicts colon cancer metastasis. *Nat Med* (2009) 15(1):59–67. doi: 10.1038/nm.1889
54. Endo A. The origin of the statins. *Atheroscler Supplements*. (2004) 5(3):125–30. doi: 10.1016/j.atherosclerosissup.2004.08.033
55. Gohlke BO, Zincke F, Eckert A, Kobelt D, Preissner S, Liebeskind JM, et al. Real-world evidence for preventive effects of statins on cancer incidence: A trans-Atlantic analysis. *Clin Trans Med* (2022) 12(2):e726. doi: 10.1002/ctm2.726
56. Carneiro CS, Hapeman JD, Nedelcu AM. Synergistic inter-clonal cooperation involving crosstalk, co-option and co-dependency can enhance the invasiveness of genetically distant cancer clones. *BMC Ecol Evolution* (2023) 23(1):20. doi: 10.1186/s12862-023-02129-7
57. AP T. Understanding the role of phenotypic heterogeneity in breast cancer. *Shodhganga* (2022).